ACS APPLIED MATERIALS & INTERFACES

www.acsami.org
Research Article

Platelet Membrane and miR-181a-5p Doubly Optimized Nanovesicles Enhance Cardiac Repair Post-Myocardial Infarction through Macrophage Polarization

Dongyue Liu,[▽] Xianyun Wang,*[,▽] Zhao Liu,[▽] Lini Ding, Mei Liu, Tianshuo Li, Shasha Zeng, Mingqi Zheng, Le Wang, Jun Zhang, Fan Zhang, Meng Li, Gang Liu,* and Yida Tang*

Cite This: *ACS Appl. Mater. Interfaces* 2025, 17, 16520−16532
Read Online

ACCESS | Metrics & More | Article Recommendations | Supporting Information

ABSTRACT: Macrophages play a crucial role in cardiac remodeling and prognosis after myocardial infarction (MI). Our previous studies have built a scalable method for preparing scaled stem cell nanovesicles (NVs) and demonstrated their remarkable reparative effects on ischemic heart disease. To further enhance the targeted reparative capabilities of the NVs toward injured myocardium, we employed a dual modification strategy involving platelet membrane coating and miR-181a-5p loading, creating a nanovesicle termed P-181-NV. This study aimed to investigate the efficacy of P-181-NV in targeted reparative interventions for damaged myocardium and to reveal the underlying mechanisms involved. After successful construction and characteristic analysis of P-181-NV, the *in vivo* tracking techniques demonstrated a significant enhancement in the targeting capacity of P-181-NV toward the injured myocardium. Moreover, P-181-NV showed marked improvements in cardiac function and remodeling as observed through ultrasound echocardiography and Masson's trichrome staining. Furthermore, P-181-NV significantly augmented myocardial cell viability, angiogenic potential, and the polarization ratio of the anti-inflammatory macrophages. The findings of this study underscore the pivotal role of platelet-membrane-coated and miR-181a-5p modified stem cell nanovesicles in facilitating postmyocardial infarction cardiac repair. By modulating macrophage polarization, P-181-NV offers a promising approach for enhancing the efficacy of targeted reparative interventions for damaged myocardium. These results contribute to our understanding of the potential of nanovesicles as therapeutic agents for cardiac repair and regeneration, presenting avenues for future research and clinical applications.

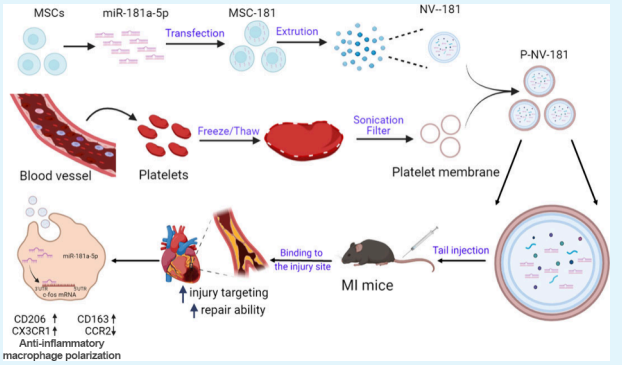

KEYWORDS: *MiR-181a-5p loaded nanovesicles, platelet membrane modification, macrophage polarization, cardiac repair, anti-inflammatory effect*

1. INTRODUCTION

Myocardial infarction (MI), commonly known as a heart attack, remains a major global health concern due to its high morbidity and mortality rate.[1] Following MI, immune-inflammatory responses play a crucial role in the reparative processes, particularly the conversion of macrophages from a pro-inflammatory to a reparative phenotype.[2,3] Despite current research showing that stem cells enhance post-MI cardiac function through immune modulation mechanisms,[4] the therapeutic efficacy of stem cell transplantation is hindered by low retention rate.[5−7] Stem-cell-derived nanovesicles (NVs) exhibit substantial promise in the next frontier in cell-free therapy.[8−10] We have made significant progress in developing a scalable methodology for the preparation of these nanovesicles, demonstrating their remarkable reparative effects in cardiac ischemia.[11,12] Stem-cell-derived NVs offer unique advantages over traditional stem cells and exosomes, such as high yield, easy storage, reduced lung retention, and extended circulation time.[13−19] However, the primary challenge lies in efficiently targeting the damaged myocardium to achieve superior myocardial repair, improved cardiac function, and reduced heart failure incidence. To address this, there is a pressing need to develop a highly efficient targeted therapeutic approach for mending the injured myocardium.

Several studies have previously highlighted the beneficial effects of platelets in increasing the homing rate of nanovesicles to the heart.[20−22] The active homing of platelet-membrane-

Received: November 7, 2024
Revised: February 24, 2025
Accepted: February 24, 2025
Published: March 11, 2025

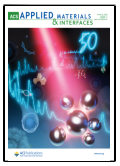

https://doi.org/10.1021/acsami.4c19325
ACS Appl. Mater. Interfaces 2025, 17, 16520−16532

optimized exosomes (P-EVs) to the site of injury is initially facilitated by their targeting interaction with endothelial vWF (von Willebrand factor) and the platelet membrane glycoprotein GPIbα. Once recruited, these P-EVs are capable of traversing the compromised endothelium to access the injury site. It has been demonstrated that extracellular vesicles coated with platelet membranes exhibited enhanced homing capabilities toward damaged myocardial tissue, resulting in a significant enhancement of cardiomyocyte viability and a substantial reduction in cardiac fibrosis.[23] The elevated surface expression of CD62P on platelet-derived extracellular vesicles (P-EVs) facilitated their engulfment by inflammatory macrophages, thereby mitigating inflammatory responses.[24] By harnessing the potential of the targeting capacity of the platelet membrane, we aim to increase the biodistribution of nanovesicles to the injured heart. Additionally, research has demonstrated that extracellular vesicles derived from mesenchymal stem cells, which overexpress miR-181a-5p, can enhance the activation and polarization of Treg cells by inhibiting c-FOS expression.[25] Consequently, this ameliorates the extent of myocardial injury resulting from ischemia-reperfusion.

Building upon these findings, we propose a hypothesis for creating a novel type of stem-cell-derived nanovesicle doubly optimized with both platelet membrane and miR-181a-5p named P-181-NV. We anticipate that P-181-NV will exhibit a remarkable reparative effect on injured myocardium. The efficacy of these nanovesicles in providing myocardial protection and reducing fibrosis will be validated using a mouse model of MI *in vivo* and a cellular oxidative stress model *in vitro*. By demonstrating the feasibility of the P-181-NV preparation method, this study aims to enhance the targeted and specific reparative effects of nanovesicles. It also provides valuable insights into the potential clinical translation and exploration of the underlying repair mechanisms of stem-cell-based therapeutic approaches for ischemic heart disease and other related conditions.

2. MATERIALS AND METHODS

2.1. Cell Culture. The mouse bone-marrow-derived mesenchymal stem cells (BM-MSCs) were purchased from Procell Life Science & Technology Co., Ltd. (catalog CP-M131), and they were cultured in Procell Mouse BM-MSC specialized medium (catalog CM-M131-100). The THP-1 cells were obtained from BeNa Culture Collection (catalog TCHu 361), and they were cultured in RPMI 1640 medium (Gibco) supplemented with 10% fetal bovine serum (FBS) (Gibco) at 37 °C with 5% CO_2. The T293 cells were obtained from BeNa Culture Collection (catalog TCHu 101), and they were cultured in high-glucose DMEM (Gibco) supplemented with 10% FBS (Gibco) at 37 °C with 5% CO_2.

2.2. Transfection. When the mouse bone marrow mesenchymal stem cell density reaches 60%, according to the instructions of Lipo3000 (Invitrogen), transfection of miR-181a-5p mimics (sequence, aaca ttcaacgctg tcggtgagt) or inhibitor and siRNA of c-FOS (sense 5′-3′, GCUGACUGAUACACUCCAATT; antisense 5′-3′, UUGGAGUGUAUCAGUCAGCTT) into the cells occurs. After transfection, the cells were placed back into the incubator and cultured for 24 h. The cells were collected for PCR validation and preparation of vesicles loaded with miR-181a-5p.

2.3. Preparation of Platelet Membrane. To prepare the platelet membrane fragments, 10 mL of mouse blood was collected and centrifuged at 2000 × g for 20 min at room temperature. The upper layer was transferred to a collection tube, and the centrifugation step (2000 × g, 20 min) was repeated. Then, 2 mL of the supernatant was mixed with an equal volume of PBS buffer containing 1 mM EDTA and 2 mM PGE1. The mixture was gently inverted and centrifuged at 800 × g for 20 min at room temperature. Approximately 3/4 of the upper layer was discarded. The remaining bottom layer was resuspended in PBS containing protease inhibitors and phosphatase inhibitors and subjected to three cycles of freezing and thawing at −80 °C. After complete thawing of the platelet extract at room temperature, centrifugation was performed at 4000 × g for 3 min, and this step was repeated five times. Finally, after centrifugation at 4000 × g for 3 min, the supernatant was discarded, and the pellet was resuspended in PBS containing protease inhibitors and phosphatase inhibitors. The resuspended pellet was washed three times with PBS and then resuspended in PBS. The platelet membrane fragment mixture was prepared by ultrasound treatment (power, 15%; ultrasound for 5 s, pause for 10 s, repeated for 20 cycles). The morphology of the platelet membrane fragments was examined by electron microscopy.

2.4. Preparation of Nanovesicles. When the fusion degree of BM-MSCs reached 80%, the cells were collected by trypsin digestion. After washing twice with PBS, the cells were collected for nanovesicle preparation. The cells were then sequentially passed through 5, 1, and 0.4 μm filters (Whatman) using LiposoFast LF-50 (Avestin, York, UK). Each filter was pressed three times, and the nanovesicles were finally obtained by passing through a 0.22 μm filter and stored at −80 °C. The protein concentration of the nanovesicles was determined using the BCA protein assay kit. The nanovesicles were mixed with platelets at a ratio of 2:1 (platelets:nanovesicles) and thoroughly mixed. The mixture was then passed through the three filters again to prepare the platelet-coated nanovesicles.

2.5. Characterization of Vesicles. The morphology, size, particle size distribution, and membrane potential of the vesicles were examined using transmission electron microscopy (TEM), nanoparticle tracking analysis, and a zeta potential analyzer. The expression level of the exosome protein marker Alix (Proteintech, 12422-1-AP), platelet membrane marker P-selectin (Proteintech, 60322-1-Ig), and the internal reference protein β-actin (Abbkine, A23910, A23720) were determined using Western blot analysis.

2.6. Flow Cytometry. When the cell density reaches 80%, the cells are collected using trypsin digestion. The cells were washed with sterile PBS 2−3 times. The cells were resuspended in 100 μL of PBS per group. Following the instructions, the flow cytometry antibodies CD206 (Proteintech, 2344972), CD163 (Proteintech, 333606), and CD68 (Proteintech, 333814) were added to the cells and incubated at room temperature for 20 min. After washing twice with PBS, the cells were resuspended in 500 μL of PBS and flow cytometry analysis was performed within 30 min.

2.7. qRT-PCR Test. To extract total RNA, we used the Trizol method. The RNA concentration was measured at a 260/230 ratio and a 260/280 ratio of the samples using a nucleic acid spectrophotometer (NanoDrop, ND1000). Reverse transcription was performed using the reverse transcription system (R323) from the manufacturer Novogene. Quantitative real-time PCR (qRT-PCR) was conducted using the qRT-PCR system (Q711) from the same manufacturer. The relative expression level of the target gene was calculated by using the $2^{-\Delta\Delta Ct}$ method.

2.8. Western Blot. To extract total protein from cells or vesicles, the BCA Protein Assay Kit (Vazyme, E112) was used to determine the protein concentration. SDS-PAGE (sodium dodecyl sulfate polyacrylamide gel electrophoresis) analysis was performed by using a Bio-Rad electrophoresis system. The proteins were then transferred from the SDS-PAGE to a PVDF membrane using a semidry transfer system. After blocking with 5% skim milk, the membranes were incubated with primary and secondary antibodies. The results were detected by using the LI-COR Odyssey CLX-0664 imaging system. The primary antibodies used included Alix (Proteintech, 12422-1-AP, 1:5000), P-selectin (60322-1-Ig, 1:2000), CD206 (Proteintech, 18704-1-AP), CD163 (Proteintech, 16646-1-AP), and β-actin (Affinity, T0022). The antimouse fluorescent secondary antibody (Abbkine, A23910) and antirabbit fluorescent secondary antibody (Abbkine, A23720) were diluted at 1:500 and incubated at room temperature in the dark for 1.5 h. After washing three times with TBST, the membranes were scanned using a LI-COR Odyssey CLX-0664 imaging system. The band

https://doi.org/10.1021/acsami.4c19325
ACS Appl. Mater. Interfaces 2025, 17, 16520−16532

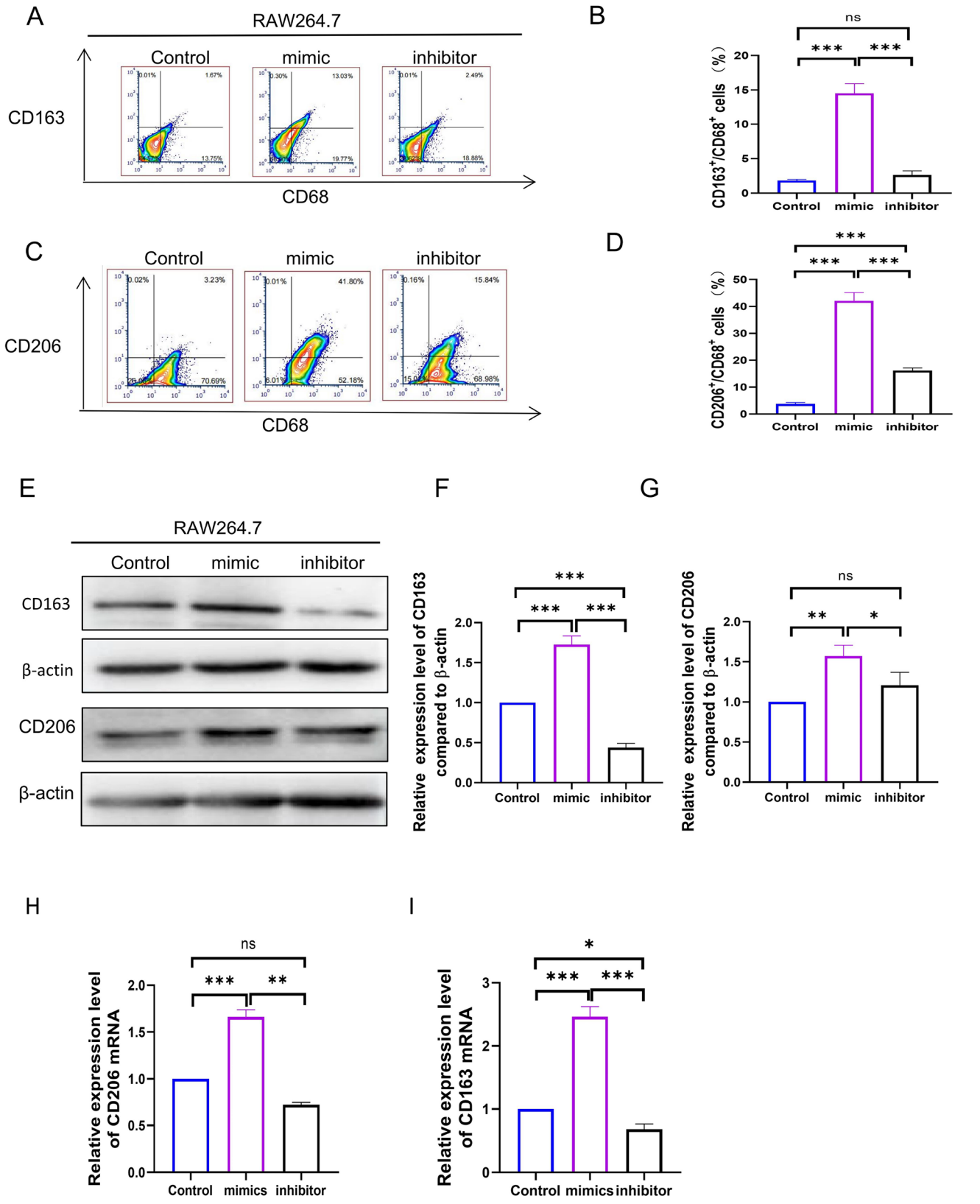

Figure 1. miR-181a-5p promoted macrophage M2 polarization. (A–D) Flow cytometry was used to analyze the polarization effect of miR-181a-5p mimics and inhibitor on macrophages, and its statistical diagram is shown. (E–G) Western blot was used to verify the effect of miR-181a-5p mimics and inhibitor on macrophage polarization, and its statistical diagram is shown. (H and I) qRT-PCR was utilized to verify the polarization effect of miR-181a-5p mimics on macrophages (mimics, miR-181a-5p mimics; inhibitor, miR-1181a-5p inhibitor).

intensities were quantified using the ImageJ imaging system, and a statistical analysis was performed on the grayscale values of the bands.

2.9. Preparation of Animal Models for Myocardial Infarction. SPF-grade C57 mice (6–8 weeks old) were purchased from the Beijing

https://doi.org/10.1021/acsami.4c19325
ACS Appl. Mater. Interfaces 2025, 17, 16520–16532

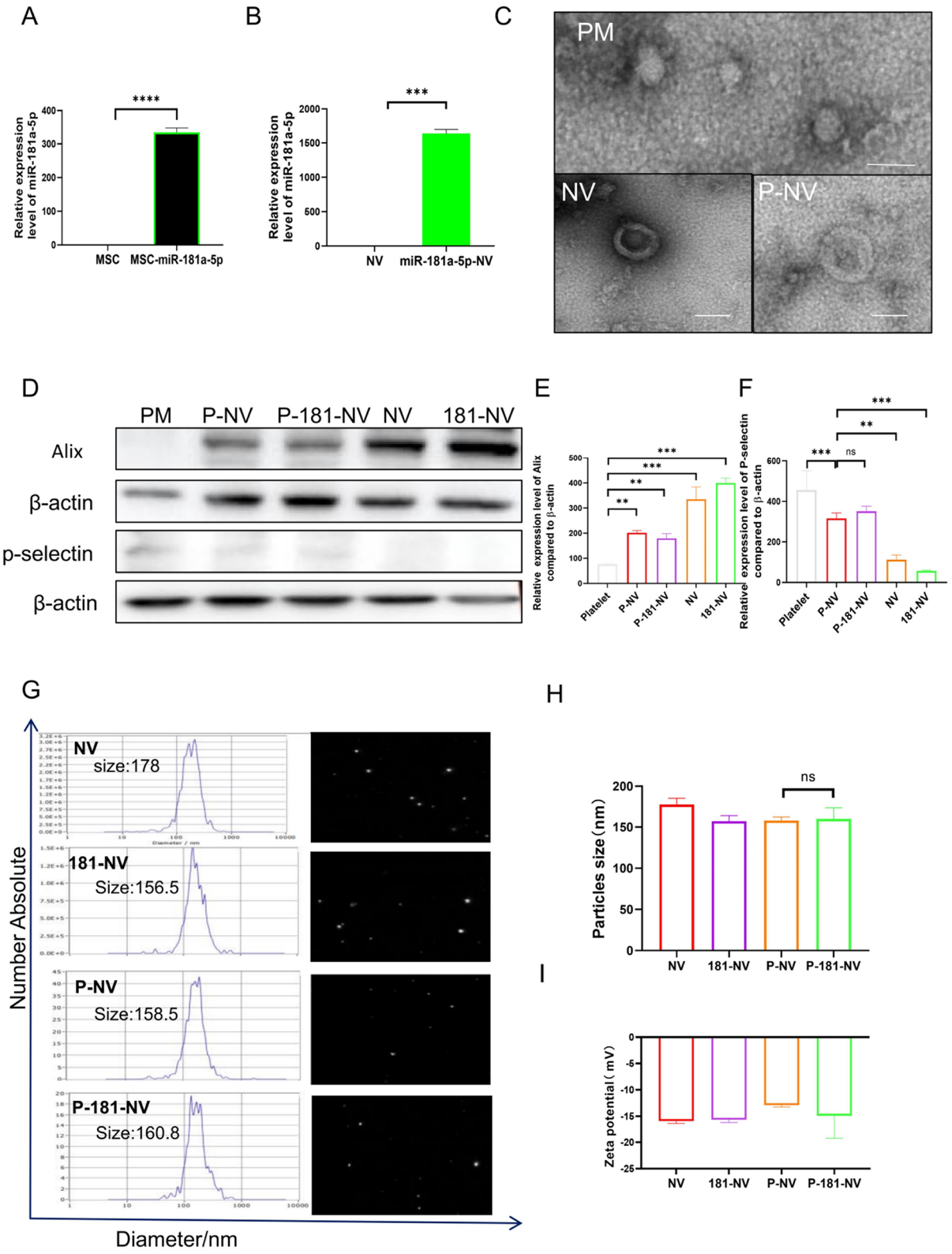

Figure 2. Morphological and biological characterization analysis of P-181-NV. (A) qRT-PCR result indicated successful transfection of miR-181a-5p at the cellular level. (B) qRT-PCR was utilized to verify the successful submission of miR181a-5p in the prepared nanovesicle with or without platelet membrane. (C) TEM indicated the electron micrographs of three kinds of vesicles of PM, NV, and P-NV (bar = 200 μm). (D−F) The expression levels of Alix, p-selectin, and β-actin were detected by Western blots, which respectively indicate the cell membrane marker of exosomes, cells, and platelet. (G and H) NTA detection showed no significant difference among different NV types. (I) The zeta potential detection showed no significant difference among different groups. Data are presented as mean ± SD from at least three independent biological replicates ($n \geq 3$) (PM, platelet membrane; NV, nanovesicles; P-NV, PM coated nanovesicles extruded from MSCs; 181-NV, nanovesicles extruded from MSCs transfected with miR-181a-5p; P-181-NV, PM coated nanovesicles extruded from miR-181a-5p modified MSCs; TEM, transmission electron microscopy; NTA, nanoparticle tracking analysis).

https://doi.org/10.1021/acsami.4c19325
ACS Appl. Mater. Interfaces 2025, 17, 16520−16532

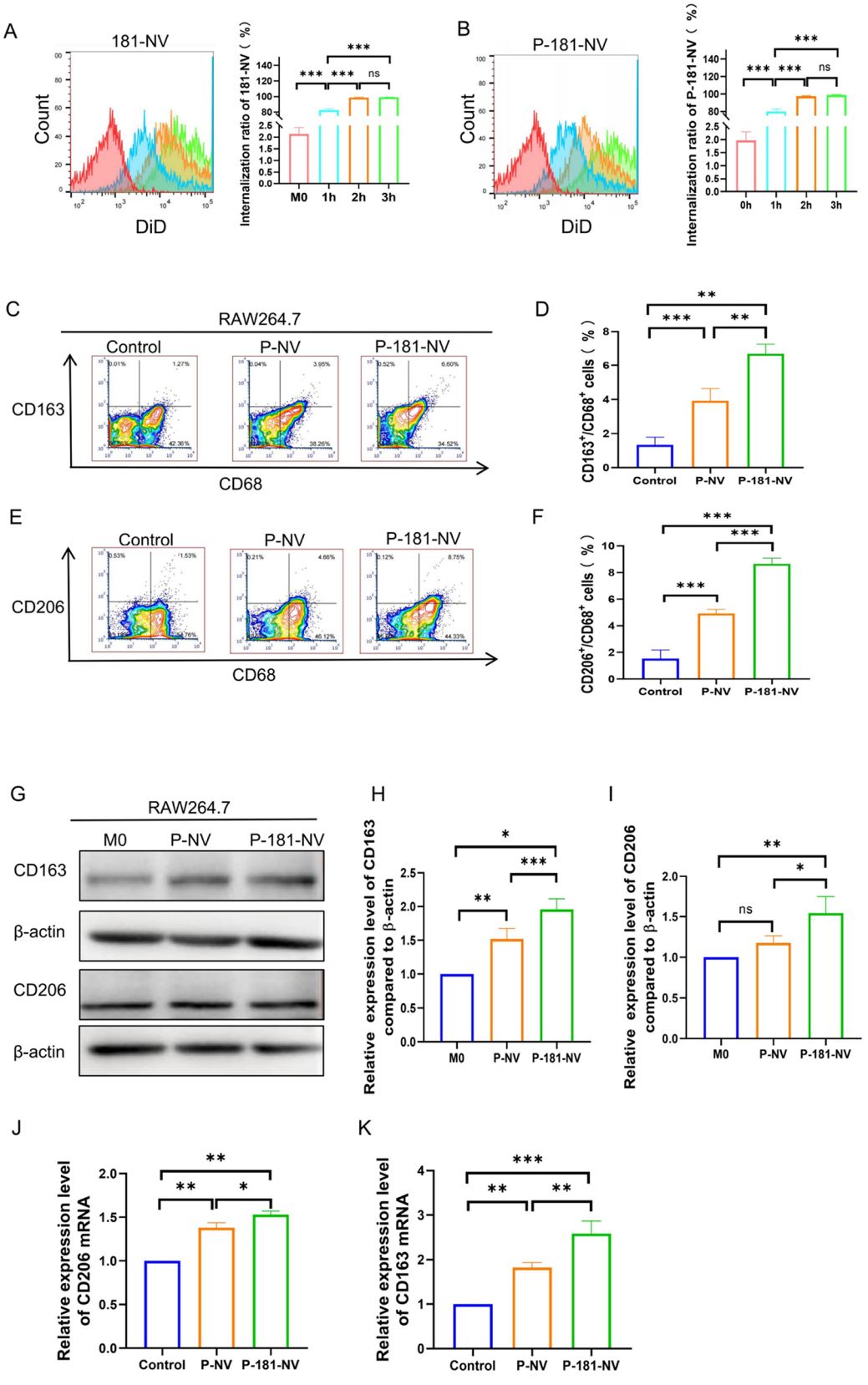

Figure 3. P-181-NV promotes macrophage polarization in the in vitro experiment. (A and B) Flow cytometry was used to detect the phagocytosis of 181-NV (A) and P-181-NV (B) vesicles by macrophages at different times. (C−F) Flow cytometry was used to analyze the polarization effect of P-181-nanovesicles on macrophages, and its statistical diagram is shown. (G−I) Western blot was used to detect the polarization effect of P-181-NV vesicles on macrophages, and its statistical diagram is shown. (J and K) qRT-PCR was utilized to verify the polarization effect of P-181-NV vesicles on macrophages (P-NV, PM coated nanovesicles extruded from MSCs; P-181-NV, PM coated nanovesicles extruded from miR-181a-5p modified MSCs).

https://doi.org/10.1021/acsami.4c19325
ACS Appl. Mater. Interfaces 2025, 17, 16520−16532

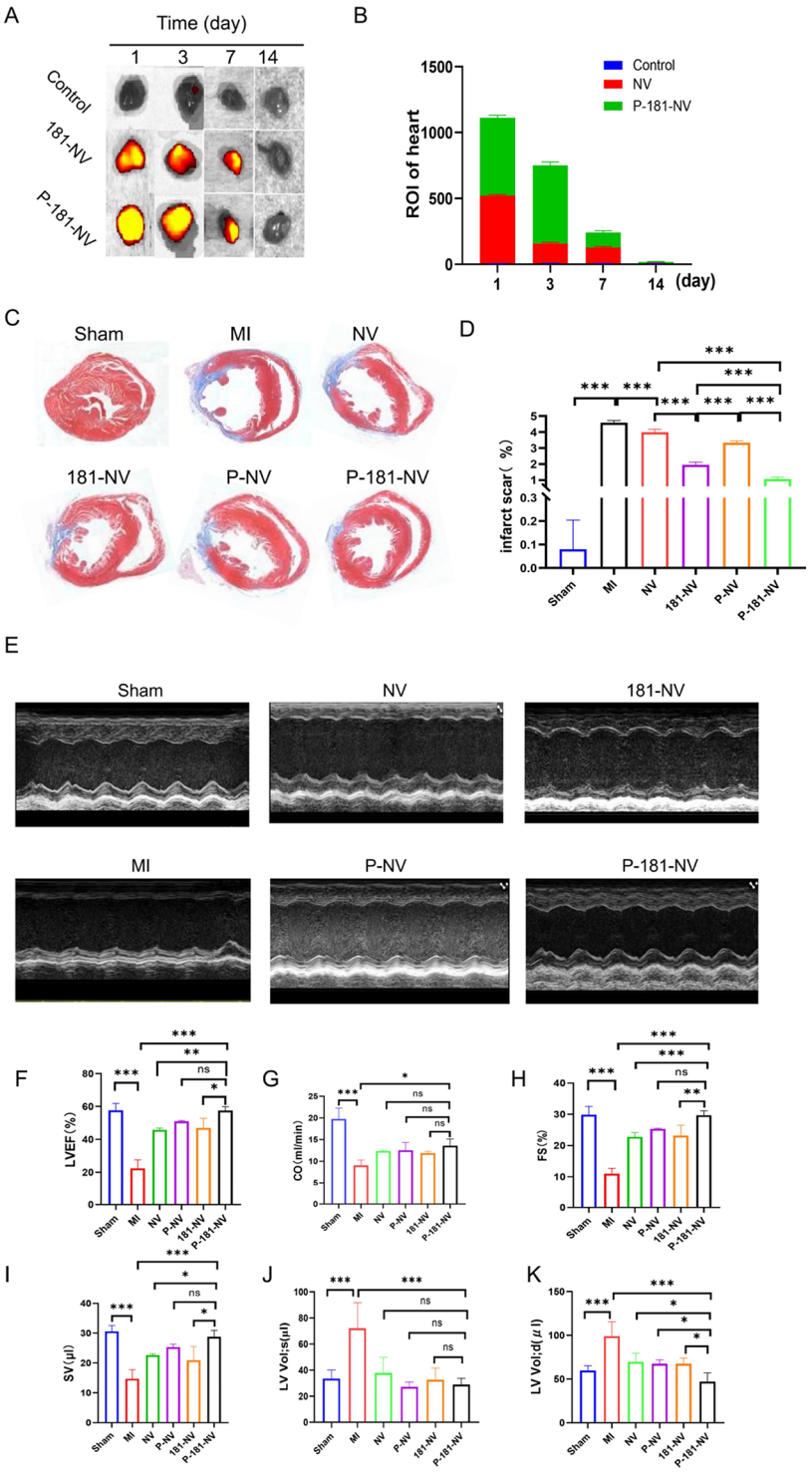

Figure 4. Biodistribution of nanovesicles and P-181-NV reduced cardiac fibrosis and improved cardiac function after MI induced heart injury. (A and B) Representative IVIS in vivo imaging data in heart were acquired at a series of time points (1, 3, 7, and 14 days) after the tail vein injection of different types of nanovesicles. (C and D) Scar size quantitation of cardiac section after Masson's trichrome staining. (E−K) Representative echocardiography images were at day 28 after nanovesicle injection. The cardiac function evaluation index including left ventricular ejection fraction (LVEF), fractional shortening (FS), cardiac output (CO), left ventricular end-systolic volume (LV Vol;s), left ventricular end-diastolic volume (LV Vol;d), and stroke volume (SV) were respectively quantified in parts (F), (G), (H), (I), (J), and (K). Data are presented as mean ± SD of at least three independent biological replicates ($n \geq 3$). ns means no significance (PM, platelet membrane; NV, nanovesicles; P-NV, PM coated nanovesicles extruded from MSCs; 181-NV, nanovesicles extruded from MSCs transfected with miR-181a-5p; P-181-NV, PM coated nanovesicles extruded from miR-181a-5p modified MSCs).

Huafukang Company. The mice were anesthetized with isoflurane gas and placed in a fixed position. A horizontal incision of approximately 5 mm was made on the left side of the sternum between the fourth ribs. The subcutaneous tissue was dissected, and the pectoral and intercostal muscles were carefully separated to expose the intercostal space. The intercostal space was opened, and the heart was gently compressed with

https://doi.org/10.1021/acsami.4c19325
ACS Appl. Mater. Interfaces 2025, 17, 16520−16532

the left-hand to make it protrude. Using an 8−0 suture, the left atrium was ligated approximately 5 mm below the left auricle, resulting in whitening of the myocardium. The chest was then closed rapidly, and the skin was sutured using a 3−0 suture material.

2.10. In Vivo Imaging and Echocardiography Test of Small Animals. First, 50 μL nanovesicles ($5\subseteq10^9$ particles/animal) labeled with DIR dye (D1220A) were injected via the tail vein at 30 min after model preparation. In vivo imaging using the PerkinElmer instrument was performed at 1, 3, 7, and 14 days to track the distribution and migration of the nanovesicles. Additionally, cardiac function was assessed using ultrasound echocardiography (VisualSonics) at 28 days, measuring parameters such as left ventricular ejection fraction (LVEF), fractional shortening (FS), cardiac output (CO), left ventricular end-systolic volume (LV Vol;s), left ventricular end-diastolic volume (LV Vol;d), and stroke volume (SV).

2.11. Cardiac Fibrosis Analysis. After injection of the nanovesicle drug at 28 days, the mouse heart tissues were collected and fixed in 4% paraformaldehyde. After fixation, the tissues were transferred to ethanol for dehydration and then embedded in paraffin for preservation. Paraffin sections were prepared for Masson's trichrome staining to visualize the fibrosis area. The fibrosis area was measured by using ImageJ software.

2.12. Tissue Fluorescence Staining. After the heart tissue was obtained, the tissue was fixed using 4% paraformaldehyde. Dehydration was performed using a sucrose gradient solution ranging from 15% to 30%, and then the tissue was embedded in an OCT and stored at −80 °C. For immunostaining, the heart tissue sections were incubated overnight at 4 °C with primary antibodies, including CD31 (Servicebio, GB113151), α-SMA (Servicebio, GB111364), Sarcomeric Alpha Actinin (Servicebio, GB11555), CX3CR1 (Servicebio, GB11861), CCR2 (Servicebio, GB11326), and CD206 (Servicebio, GB113497). Subsequently, fluorescent secondary antibodies (Servicebio, GB22403, and GB21303) and TSA amplification (Servicebio, G1222, G1223) were applied sequentially, followed by antigen retrieval. Finally, the sections were counterstained with DAPI and mounted on a coverslip. The slides were observed under a microscope (NIKON Eclipse Ci).

2.13. Statistical Analysis. In this study, data analysis and graphing were performed using Prism statistical software. Quantitative data are presented as the mean ± standard deviation (mean ± SD). For comparisons between two groups, the t test was used, while for comparisons among multiple groups, one-way analysis of variance (ANOVA) was conducted. The significance level was set at $\alpha = 0.05$, and differences with a P-value less than 0.05 ($P < 0.05$) were considered statistically significant.

3. RESULTS

3.1. miR-181a-5p Promoted the Macrophage Polarization. RAW264.7 cells and THP-1 cells were used in this part to explore the regulating ability of miR-181a-5p for anti-inflammatory macrophage polarization. RAW264.7 cells were divided into three groups (control, mimics, and inhibitor) and subjected to different treatments. After 48 h of treatment, flow cytometry showed that a significant increase in the proportion of anti-inflammatory macrophage in the miR-181a-5p group (Figures 1A−1D and Figures S1A−S1D). Western blot analysis and qRT-PCR demonstrated a significant upregulation of the expression levels of anti-inflammatory macrophages CD163 and CD206 in the P-181-NV group (Figures 1E−1I, Figures S1E−S1G, and Figures S1J and S1K). These findings indicate that miR-181a-5p exerts a promotion effect on the M2 macrophage polarization. Consequently, based on previous research and our findings on miR-181a-5p, we aimed to engineer nanovesicles with highly efficient targeting of damaged myocardium.

3.2. Fabrication and Characterization of P-181-NV. First, miR-181a-5p was transfected into MSCs to obtain miR-181a-5p enriched MSCs (Figure 2A), which were then extruded utilizing the extruder. qRT-PCR results showed a significant increase of miR-181a-5p in 181-NV (Figure 2B). Following, platelet membranes were incorporated to establish P-181-NV. TEM revealed that P-181-NV exhibited a double-layered membrane structure (Figure 2C). Western blot analysis in Figures 2D− 2F revealed an increasing expression level of p-selectins in P-181-NV, indicating the successful preparation of P-181-NV. NTA revealed that the diameter of the engineered nanovesicles was approximately 100−200 nm (Figures 2G and 2H). Zeta potential results in Figure 2I showed no significant differences among the four groups, which varied from 10 to 15 mV. These results demonstrated the successful construction and production of the P-181-NV.

3.3. Macrophage Polarization after P-181-NV Treatment. The anti-inflammatory macrophage polarization ability of P-181-NV was evaluated. First, NVs labeled with DiD were cocultured with macrophages for different time periods, and the phagocytic efficiency of macrophages was measured using flow cytometry. The results showed that almost all the vesicles were engulfed by macrophages 2 h post coincubation, demonstrating their effective uptake by macrophages (Figures 3A and 3B). Next, RAW264.7 and THP-1 cells were used to verify the ability of the vesicles to promote macrophage polarization. RAW264.7 cells were divided into three groups (control, P-NV, and P-181-NV) and subjected to different treatments. After 48 h of treatment, flow cytometry showed that a significant increase in the proportion of anti-inflammatory macrophage in the P-181-NV group (Figures 3C−3F and Figures S2A−S2D). Western blot and qRT-PCR results both demonstrated a significant upregulation of the expression level of CD163 and CD206 after P-181-NV stimulation (Figures 3G−3K, Figures S2E−S2G, and Figures S2J and S2K).

3.4. Biodistribution of Nanovesicles after MI Induced Heart Injury. To assess the targeting ability of the P-181-NV toward the injured myocardium, we intravenously administered DiR-labeled nanovesicles to mice 24 h post MI injury. The MI mice were randomly divided into three groups: sham (PBS), 181-NV, and P-181-NV. The ability of the vesicles to home to the injured myocardium was evaluated on days 1, 3, 7, and 14 post administration (Figures 4A and 4B). The results demonstrated a significant increase in the homing rate of vesicles to the heart in the P-181-NV group on days 1, 3, and 7. On day 14, the fluorescence signal of vesicles in the heart in all groups almost disappeared (Figure 4A). Notably, on day 14, the retention rate of fluorescence signals in the liver, spleen, lung, and kidney were reduced in the P-181-NV group (Figures S3A−S3D).

These findings indicated that P-181-NV effectively reduced the retention rate in the liver while significantly increasing the retention rate in the heart. This remarkable targeting capability lays a crucial foundation for further exploring the functional characteristics of P-181-NV in repairing the injured myocardium.

3.5. Therapeutic Effect of P-181-NV in Mice with MI. Mice were euthanized on day 28 and cardiac pathological sections were prepared. Masson's staining demonstrated that P-181-NV significantly reduced the area of cardiac fibrosis (Figures 4C and 4D). Moreover, the echocardiography results revealed that the P-181-NV group exhibited significantly improved LVEF, FS, and SV when compared to the other groups, except P-NV (Figures 4E−4K). These findings collectively indicate a notable capacity of P-181-NV in cardiac fibrosis inhibition and cardiac function provement in MI mice.

https://doi.org/10.1021/acsami.4c19325
ACS Appl. Mater. Interfaces 2025, 17, 16520−16532

3.6. Angiogenesis and Inflammation after P-181-NV Treatment.

To investigate the pro-angiogenic ability of P-181-NV, immunofluorescent experiments were performed which revealed that P-181-NV significantly increased both the CD31 and α-SMA expression on days 7 and 14 (Figures S4A–S4F), indicating a significantly pro-angiogenic function of P-181-NV in the injured myocardium following MI.

The anti-inflammatory macrophage markers of CX3CR1 and CD206 and the pro-inflammatory macrophage phenotype of CCR2 were used to explore the immunoregulatory effect of P-181-NV. The results demonstrated that on days 3 and 7, P-181-NV treatment significantly increased the percentage of CX3CR1 (Figures 5A–5C and 5D–5F, respectively) and CD206 positive

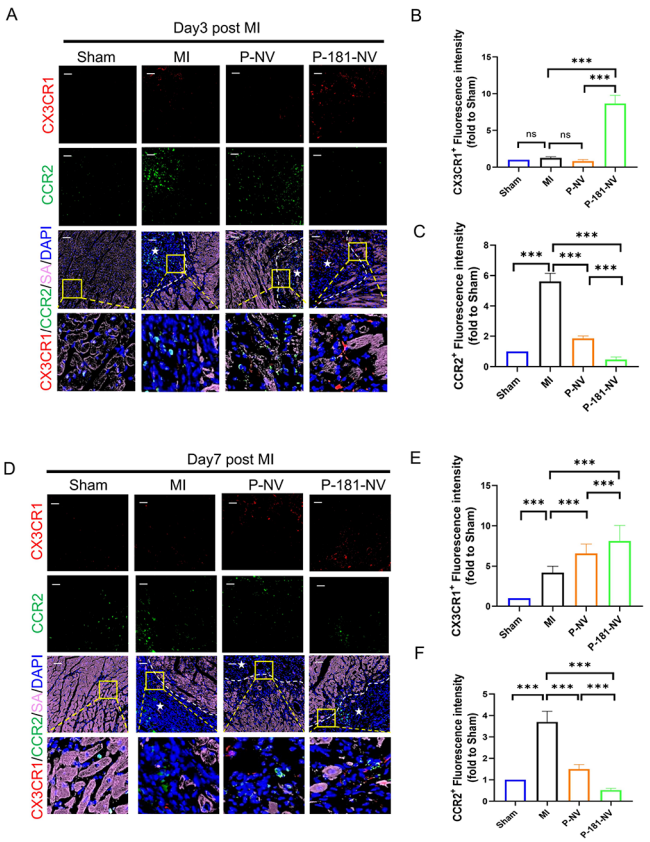

Figure 5. P-181-NV promotes the differentiation of CX3CR1 positive anti-inflammatory macrophage on days 3 and 7 post MI. The fluorescence intensity of CX3CR1 positive anti-inflammatory macrophage and CCR2+ positive proinflammatory macrophages were respectively detected and qualified on days 3 (A–C) and 7 (D–F) post MI using the immunofluorescence method (bar = 50 μm). Data are presented as mean ± SD of at least three independent biological replicates ($n \geq 3$). ns means no significance (P-NV, PM coated nanovesicles extruded from MSCs; P-181-NV, PM coated nanovesicles extruded from miR-181a-5p modified MSCs).

cells (Figures 6A–6D) compared to the MI and P-NV groups. On day 14, CD206 was still significantly more highly expressed in the P-181-NVgroup compared with the MI and P-NV groups (Figures 6E and 6F), while the CX3CR1-positive cell percentage showed no significant difference among them (Figures S6A–S6C). These findings suggest that P-181-NV can significantly promote the polarization of M2 anti-inflammatory macrophages, indicating that P-181-NV can effectively promote M2 macrophage polarization.

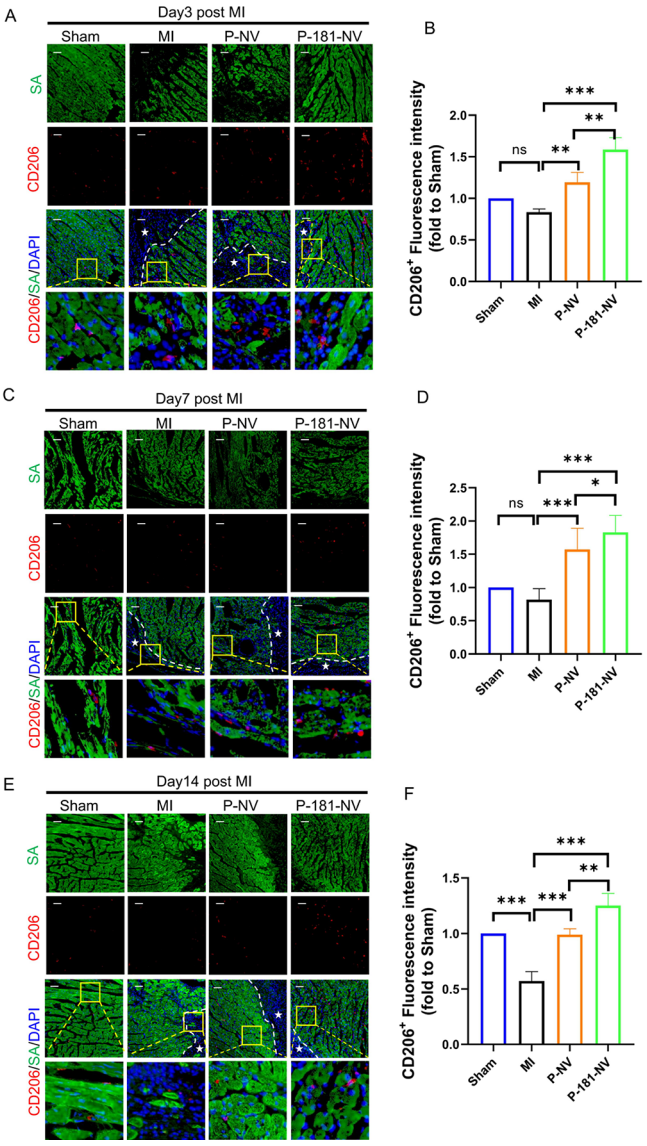

Figure 6. P-181-NV promotes the M2 macrophage differentiation on days 3, 7, and 14 post MI. The fluorescence intensity of the CD206 positive M2 macrophage was respectively detected using immunofluorescence and qualified on day 3 (A and B), 7 (C and D), and 14 (E and F) post MI (bar = 50 μm). Data are presented as mean ± SD of at least three independent biological replicates ($n \geq 3$). ns means no significance (P-NV, PM coated nanovesicles extruded from MSCs; P-181-NV, PM coated nanovesicles extruded from miR-181a-5p modified MSCs).

3.7. Mechanism of P-181-NV Promoted Macrophage M2 Polarization.

To further investigate the mechanism by which P-181-NV promotes anti-inflammatory macrophage polarization, we used bioinformatics tools, including miRDB, Pictar, Targetscan, and miRwalk to predict the target genes of miR-181a-5p. The intersection of the predicted target genes and inflammation genes from the Gene Ontology database was taken, resulting in seven candidate downstream targets (Figure 7A). Based on literature reports of the regulatory role of miR-181a-5p/c-FOS in dendritic cells' anti-inflammatory effects, we selected c-FOS as the target gene of miR-181 for validation. Dual-luciferase reporter assays demonstrated that miR-181a-5p significantly inhibited the wild-type c-FOS level but had no significant inhibitory effect on the mutant type (Figure 7B),

https://doi.org/10.1021/acsami.4c19325
ACS Appl. Mater. Interfaces 2025, 17, 16520–16532

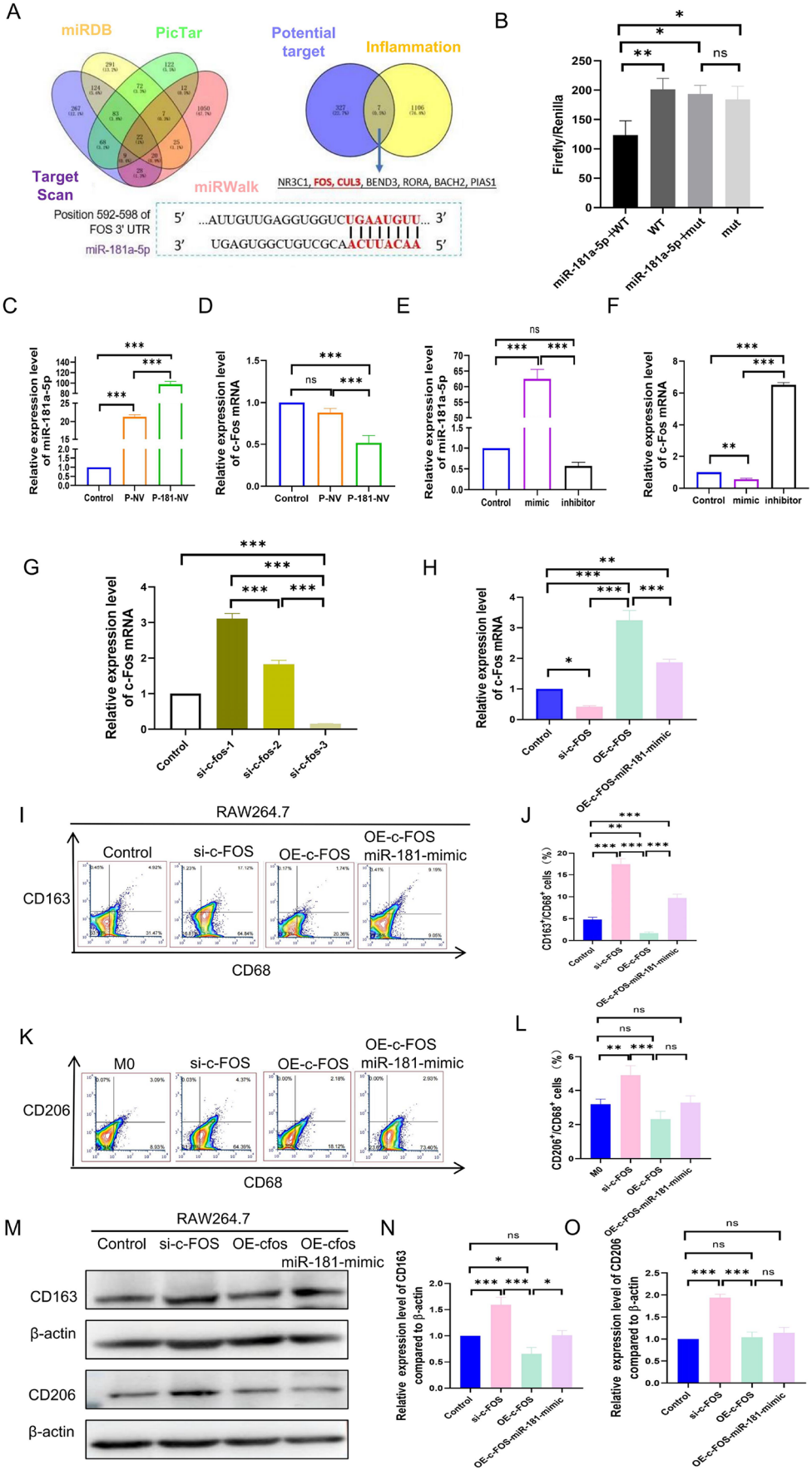

Figure 7. P-181-NV promoted macrophage M2 polarization by targeting inhibition of c-Fos mRNA. (A) miRDB, PicTar, TargetScan, and miRWalk were used to predict the potential target genes of miR-181a-5p. Seven candidate genes were acquired from the intersection of the potential target genes

https://doi.org/10.1021/acsami.4c19325
ACS Appl. Mater. Interfaces 2025, 17, 16520−16532

Figure 7. continued

and inflammation genes from the Gene Ontology Resourse database. (B) The relationship between miR-181a-5p and c-Fos was verified by a double luciferase report experiment. (C and D) qRT-PCR was utilized to verify the successful submission of miR-181a-5p in the prepared nanovesicle with or without platelet membrane and evaluate the effect of P-181-NV and P-NV on the expression of c-Fos in Raw cells. (E and F) qRT-PCR indicated the transfection efficiency of mimics and inhibitor in Raw cells and evaluated the effect of mimics and inhibitor on the expression of c-Fos in Raw cells. (G) The inhibitory effect of different types of c-Fos-siRNA were detected. (H) qRT-PCR was used to assess the impact of c-Fos-siRNA and OE-c-Fos on the expression of c-Fos in Raw cells. (I and J) qRT-PCR was utilized to verify the polarization effect of c-Fos-siRNA and OE-c-Fos on macrophages. (K−N) Flow cytometry was used to analyze the polarization effect of c-Fos-siRNA and OE-c-Fos on macrophages, and its statistical diagram is shown. (O−Q) Western blot was used to verify the effect of c-Fos-siRNA and OE-c-Fos on macrophage polarization, and its statistical diagram is shown (mimics, miR-1181a-5p mimics; inhibitor, miR-1181a-5p inhibitor; c-Fos-siRNA, inhibition of c-Fos expression; OE-c-Fos, overexpression of c-Fos).

indicating that miR-181a-5p can target and suppress c-FOS gene expression. PCR analysis (Figures 7C and 7D, Figures S1H−S1I, and Figures S2H−S2I) was inferred that c-FOS may mediate the anti-inflammatory macrophage polarization regulated by P-181-NV. Then, we verified that P-181-NV could significantly inhibit the expression level of the c-FOS gene (Figure 7D). qRT-PCR results further demonstrated that miR-181a-5p can inhibit the expression level of c-FOS (Figures 7E and 7F). these results showed that P-181-NV could significantly decrease the expression of c-FOS on days 3 and 7 (Figures 8A−8F), indicating that P-181-NV could significantly suppress c-FOS expression in the injured myocardium.

Subsequently, siRNA interference was used to knock down c-FOS, and qRT-PCR results showed that c-FOS-siRNA-3 significantly inhibited the elevation of c-FOS level (Figures 7G and 7H and Figure S5H). Flow cytometry showed that with a significant increase in the proportion of anti-inflammatory macrophage in the c-FOS-siRNA group, the expression level of CD163 was significantly decreased in the OE-c-FOS group compared to the control group (Figures 7K−7N and Figures S5A−S5D). Knock-down of c-FOS using siRNA remarkably promotes the expression level of CD163 and CD206 either compared to the control group or the OE-c-FOS group, while the OE-c-FOS-miR-181a-5p group effectively rescued their expression compared to the OE-c-FOS group (Figures 7I and 7J, Figures 7O−7Q, Figures S5E−S5G, and Figures S5I and S5J). These results indicate that P-181-NV can significantly inhibit c-FOS expression in macrophages, and the decrease in the c-FOS level is associated with anti-inflammatory macrophage polarization. In summary, P-181-NV can promote anti-inflammatory macrophage polarization through the targeted regulation of c-FOS, thereby exerting an anti-inflammatory regulatory effect.

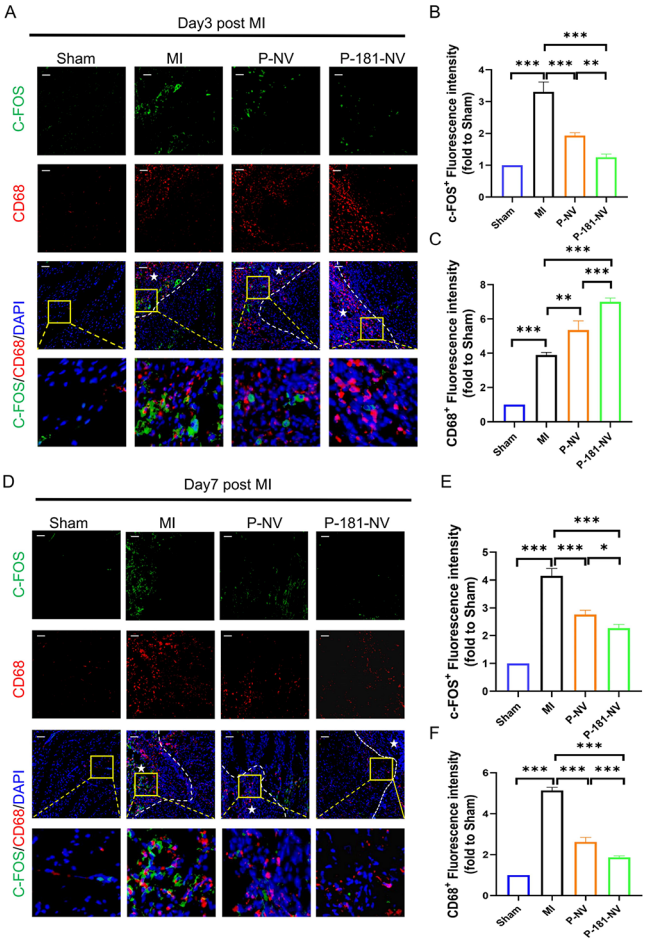

Figure 8. P-181-NV suppresses the expression of c-FOS on macrophages on days 3 and 7 post MI. The fluorescence intensity of c-FOS positive cell and CD68 positive cell were respectively detected and qualified on days 3 (A−C) and 7 (D−F) post MI using the immunofluorescence method (bar = 50 μm). Data are presented as mean ± SD of at least three independent biological replicates ($n \geq 3$). ns means no significance (P-NV, PM coated nanovesicles extruded from MSCs; P-181-NV, PM coated nanovesicles extruded from miR-181a-5p modified MSCs).

4. DISCUSSION

Currently, immune regulation plays an increasingly important role in the acute injury and repair processes of ischemic heart disease.[26] Therefore, exploring effective intervention strategies for the inflammatory response in the acute phase of ischemic heart disease is an important issue that needs to be urgently addressed. In this work, we effectively generated platelet-coated nanovesicles with a high expression level of miR-181a-5p. Unlike P-NV or 181-NV groups, P-181-NV has a high targeting efficiency and the capacity to mend the heart. Via targeting c-FOS, P-181-NV controlled the anti-immune inflammatory response and macrophage polarization, resulting in their evident cardiac repair effect. These results provide a crucial basis for its clinical translational use.

The preparation of P-181-NV includes three steps: MSC transfection with miR-181a-5p, manufacture of platelet membranes, and production of doubly modified nanovesicles. According to clinical research, stem cell transplantation can greatly improve heart function and LVEF with no obvious negative adverse effects.[27,28] MSCs derived extracellular vesicles could significantly elevate LVEF, reduce infarct size, and improve ventricular wall thickness with no significant immune response, hematological profiles, and abnormal liver and kidney function, indicating the safety and effectiveness of exosomes treatment in both mouse and pig MI models.[29] Furthermore, the components of MSC extruded nanovesicles closely resembled the extracellular vesicles, and no negative effects presented in the

https://doi.org/10.1021/acsami.4c19325
ACS Appl. Mater. Interfaces 2025, 17, 16520−16532

NV injection group post MI using a blood biochemical test.[11,12] Additionally, it has been demonstrated that the microparticles with platelet membrane and IL-1β antibody greatly reduce the inflammatory response at cardiac injury sites, preventing irreversible cardiac remodeling and the development of heart failure.[30] Consequently, given the established safety profile of platelet membrane-modified nanoparticles[31,32] and the effective immunomodulatory function of miR-181a-5p,[25] the platelet membrane and miR-181a-5p doubly modified nanovesicles were established here to repair the damaged cardiac.[23] Thus, P-181-NV has dramatically positive safety and feasibility to treat MI, which will lay a strong basis for P-181-NVs' future application.

Additionally, in vivo distribution data in Figures 4A and 4B indicated P-181-NV peaked in the heart on day 1, gradually decreased on the third and seventh days following injection, and were completely metabolized on day 14. More importantly, the cardiac retention rate of P-181-NV showed a more significant enhancement than the other groups (Figures 4A and 4B). Nonetheless, the higher distribution rate of P-181-NV in the liver and lung tissue still exist (Figures S3A−S3D). Nanovesicles either modified by cardiac targeted peptides (CTP) or by biochemical material could not avoid the high liver and lung retention rate also including the inhaled administration techniques application.[33−36] So, the liver and lung retention rate in the nanomedicine field still remains a challenging scientific problem deserving further exploration.

P-181-NV also displayed a strong repair effect toward injured myocardium in addition to its safety. miR-181a has been validated across numerous studies in enhancing the immunoregulation role of ischemic heart disease. For example, miR-181a delivered by extracellular vesicles of MSCs could curb oxLDL-induced dendritic cell activation, mitigate inflammatory responses, and activate Treg cells through inhibiting c-FOS activity.[37] miR-181a could upregulate FoxP3 expression and IL-10 secretion to dampen immune responses and downregulate TNF-α and IL-6 levels, thereby increasing the proportion of Treg cells.[38,39] Moreover, miR-181a could promote Treg cell polarization by blocking the TGF-β/Smad7 pathway, resulting in better immune reparative effects on ischemic heart disease.[40] Therefore, the promotion effect of miR-181a-5p on M2 macrophage polarization (Figure 1) was strongly proved in this study. Then, bioinformatics analysis (Figure 7A) and dual-luciferase reporter assays (Figure 7B) showed that c-FOS could be targeting inhibited by miR-181a-5p. Figures 7H−7Q showed an obvious promotion phenomenon of anti-inflammatory macrophage polarization after c-FOS knock down, which was consistent with the previous study about the c-FOS-siRNA modulated anti-inflammatory action.[41] However, we did not conduct an in-depth analysis on the detailed downstream mechanism of c-FOS, which will be conducted in our future study.

In summary, P-181-NV, characterized by platelet coating and high expression of miR-181a-5p, has demonstrated exceptional cardiac tropism and reparative efficacy. P-181-NV was capable of modulating macrophage polarization, thereby dampening the immune response associated with ischemic heart disease. P-181-NV demonstrated a favorable safety profile with a minimal risk of adverse reactions in ischemic myocardial repair. In conclusion, our findings may pave the way for novel applications of stem cell vesicles, offering innovative avenues for the utilization of stem cell nanovesicles in cardiac disease management.

5. CONCLUSIONS

Based on our previous stem cell nanovesicle technology, we successfully prepared highly efficient targeted nanovesicles P-181-NV modified by platelet membrane and miR-181a-5p displaying higher targeted retention rate and strong repair effects toward injured myocardium. miR-181a-5p delivered by P-181-NV could significantly promote the polarization of anti-inflammatory macrophages via targeting inhibition of c-FOS to repair damaged myocytes following MI. This study will establish an important theoretical foundation for the future clinical application of MSC-derived nanovesicles.

■ ASSOCIATED CONTENT

Supporting Information

The Supporting Information is available free of charge at https://pubs.acs.org/doi/10.1021/acsami.4c19325.

Additional data showing THP-1 macrophage M2 polarization, miR-181a-5p promoted macrophage M2 polarization (Figure S1), P-181-NV promote macrophage polarization in vitro experiment (Figure S2), biodistribution of nanovesicles in liver, spleen, lung and kidney after being injected to the MI mice (Figure S3), P-181-NV promoting angiogenesis on days 7 and 14 post MI (Figure S4), P-181-NV promoting macrophage M2 polarization by targetting inhibition of c-Fos mRNA (Figure S5), and P-181-NV promoting the differentiation of CX3CR1 positive anti-inflammatory macrophage on day 14 post MI (Figure S6) (PDF)

■ AUTHOR INFORMATION

Corresponding Authors

Xianyun Wang − *Department of Cardiovascular Medicine, The First Hospital of HeBei Medical University, Shijiazhuang 050031 Hebei Province, China; Hebei Provincial Key Laboratory of Cardiac Injury Repair Mechanism Study, Shijiazhuang 050031 Hebei Province, China;* orcid.org/0000-0003-2224-4770; Phone: +86-18633889197; Email: wangxianyun_mbb@hebmu.edu.cn

Gang Liu − *Department of Cardiovascular Medicine, The First Hospital of HeBei Medical University, Shijiazhuang 050031 Hebei Province, China; Hebei Provincial Key Laboratory of Cardiac Injury Repair Mechanism Study, Shijiazhuang 050031 Hebei Province, China; Hebei International Joint Research Center for Structural Heart Disease, Shijiazhuang 050031 Hebei Province, China*; Phone: +86-18633889897; Email: cardio2004@hebmu.edu.cn

Yida Tang − *Department of Cardiovascular Medicine, The First Hospital of HeBei Medical University, Shijiazhuang 050031 Hebei Province, China; Department of Cardiology, Peking University Third Hospital, Beijing 100191, China*; Phone: +86-13901010211; Email: 57303411@hebmu.edu.cn

Authors

Dongyue Liu − *Department of Cardiovascular Medicine, The First Hospital of HeBei Medical University, Shijiazhuang 050031 Hebei Province, China; Hebei Provincial Key Laboratory of Cardiac Injury Repair Mechanism Study, Shijiazhuang 050031 Hebei Province, China;* orcid.org/0000-0001-7275-4985

Zhao Liu − *Traditional Chinese Medicine Processing Technology Innovation Center of Hebei Province, School of*

https://doi.org/10.1021/acsami.4c19325
ACS Appl. Mater. Interfaces 2025, 17, 16520−16532

Pharmacy, Hebei University of Chinese Medicine, Shijiazhuang 050091, China; International Joint Research Center on Resource Utilization and Quality Evaluation of Traditional Chinese Medicine of Hebei Province, Shijiazhuang 050091, China

Lini Ding − *Department of Cardiovascular Medicine, The First Hospital of HeBei Medical University, Shijiazhuang 050031 Hebei Province, China; Hebei Provincial Key Laboratory of Cardiac Injury Repair Mechanism Study, Shijiazhuang 050031 Hebei Province, China*

Mei Liu − *Department of Cardiovascular Medicine, The First Hospital of HeBei Medical University, Shijiazhuang 050031 Hebei Province, China; Hebei Provincial Key Laboratory of Cardiac Injury Repair Mechanism Study, Shijiazhuang 050031 Hebei Province, China*

Tianshuo Li − *Department of Cardiovascular Medicine, The First Hospital of HeBei Medical University, Shijiazhuang 050031 Hebei Province, China; Hebei Provincial Key Laboratory of Cardiac Injury Repair Mechanism Study, Shijiazhuang 050031 Hebei Province, China*

Shasha Zeng − *Department of Cardiovascular Medicine, The First Hospital of HeBei Medical University, Shijiazhuang 050031 Hebei Province, China; Hebei Provincial Key Laboratory of Cardiac Injury Repair Mechanism Study, Shijiazhuang 050031 Hebei Province, China*

Mingqi Zheng − *Department of Cardiovascular Medicine, The First Hospital of HeBei Medical University, Shijiazhuang 050031 Hebei Province, China; Hebei Provincial Key Laboratory of Heart and Metabolism, Shijiazhuang 050031 Hebei Province, China*

Le Wang − *Department of Cardiovascular Medicine, The First Hospital of HeBei Medical University, Shijiazhuang 050031 Hebei Province, China; Hebei Provincial Key Laboratory of Heart and Metabolism, Shijiazhuang 050031 Hebei Province, China*

Jun Zhang − *Department of Cardiovascular Medicine, The First Hospital of HeBei Medical University, Shijiazhuang 050031 Hebei Province, China; Hebei Provincial Key Laboratory of Cardiac Injury Repair Mechanism Study, Shijiazhuang 050031 Hebei Province, China*

Fan Zhang − *Department of Cardiovascular Medicine, The First Hospital of HeBei Medical University, Shijiazhuang 050031 Hebei Province, China; Hebei Provincial Key Laboratory of Cardiac Injury Repair Mechanism Study, Shijiazhuang 050031 Hebei Province, China*

Meng Li − *College of Pharmacy, Key Laboratory of Innovative Drug Development and Evaluation, Hebei Medical University, Shijiazhuang 050017, China;* orcid.org/0000-0002-8348-6768

Complete contact information is available at: https://pubs.acs.org/10.1021/acsami.4c19325

Author Contributions

[▽]D.L., X.W., and Z.L. contributed equally to this work.

Notes

The authors declare no competing financial interest.

■ ACKNOWLEDGMENTS

The present study was financially supported in part by the Science and Technology Support Program of Hebei Province (Grants 203777117D and 22377719D to G.L.), the National Natural Science Foundation of China (Grant 82200276 to X.W.), the Clinical Medical Talents Project sponsored by Hebei Province (Grants LS202209 to X.W. and LS202201 to G.L.), the Hebei Natural Science Foundation (Grants H2021206399 to M.Z., H2021206031 to L.W., and H2022206295 to G.L.), the Introduced Overseas Students Funding Project of Hebei Province (Grant C20210347 to X.W.), the Graduate Students Innovation Capability Training Funding Project of Hebei Province (Grant CXZZBS2024127 to D.L.), the "14th Five-Year Plan" clinical medicine Innovation Research Team Project of Hebei Medical University (Grants 2022LCTD-A2 to G.L. and 2023LCTD-B7 to X.W.), and the Chinese Medicine Scientific Research Project (Grant 2024030 to X.W.). The funding bodies had no involvement in the design of the study, collection, analysis or interpretation of data, or manuscript writing. Illustrations were created with BioRender.

■ REFERENCES

(1) Alves, L.; Ziegelmann, P. K.; Ribeiro, V.; Polanczyk, C. Hospital Mortality from Myocardial Infarction in Latin America and the Caribbean: Systematic Review and Meta-Analysis. *Arq Bras Cardiol* **2022**, *119*, 970−978.

(2) Peet, C.; Ivetic, A.; Bromage, D. I.; Shah, A. M. Cardiac monocytes and macrophages after myocardial infarction. *Cardiovasc. Res.* **2020**, *116*, 1101−1112.

(3) Wang, Z.; Yu, J.; Wu, J.; Qi, F.; Wang, H.; Wang, Z.; Xu, Z. Scutellarin protects cardiomyocyte ischemia-reperfusion injury by reducing apoptosis and oxidative stress. *Life Sci.* **2016**, *157*, 200−207.

(4) Vandergriff, A.; Huang, K.; Shen, D.; Hu, S.; Hensley, M. T.; Caranasos, T. G.; Qian, L.; Cheng, K. Targeting regenerative exosomes to myocardial infarction using cardiac homing peptide. *Theranostics* **2018**, *8*, 1869−1878.

(5) Guo, Y.; Yu, Y.; Hu, S.; Chen, Y.; Shen, Z. The therapeutic potential of mesenchymal stem cells for cardiovascular diseases. *Cell Death Dis* **2020**, *11*, 349.

(6) Turner, D.; Rieger, A. C.; Balkan, W.; Hare, J. M. Clinical-based Cell Therapies for Heart Disease-Current and Future State. *Rambam Maimonides Med. J.* **2020**, *11*, No. e0015.

(7) Barbash, I. M.; Chouraqui, P.; Baron, J.; Feinberg, M. S.; Etzion, S.; Tessone, A.; Miller, L.; Guetta, E.; Zipori, D.; Kedes, L. H.; Kloner, R. A.; Leor, J. Systemic delivery of bone marrow-derived mesenchymal stem cells to the infarcted myocardium: feasibility, cell migration, and body distribution. *Circulation* **2003**, *108*, 863−868.

(8) Ilahibaks, N. F.; Lei, Z.; Mol, E. A.; Deshantri, A. K.; Jiang, L.; Schiffelers, R. M.; Vader, P.; Sluijter, J. P. G. Biofabrication of Cell-Derived Nanovesicles: A Potential Alternative to Extracellular Vesicles for Regenerative Medicine. *Cells* **2019**, *8*, 1509.

(9) Lee, H.; Cha, H.; Park, J. H. Derivation of Cell-Engineered Nanovesicles from Human Induced Pluripotent Stem Cells and Their Protective Effect on the Senescence of Dermal Fibroblasts. *Int. J. Mol. Sci.* **2020**, *21*, 343.

(10) Wang, X.; Tang, Y.; Liu, Z.; Yin, Y.; Li, Q.; Liu, G.; Yan, B. The Application Potential and Advance of Mesenchymal Stem Cell-Derived Exosomes in Myocardial Infarction. *Stem Cells Int.* **2021**, *2021*, 5579904.

(11) Wang, X.; Hu, S.; Li, J.; Zhu, D.; Wang, Z.; Cores, J.; Cheng, K.; Liu, G.; Huang, K. Extruded Mesenchymal Stem Cell Nanovesicles Are Equally Potent to Natural Extracellular Vesicles in Cardiac Repair. *ACS Appl. Mater. Interfaces* **2021**, *13*, 55767−55779.

(12) Wang, X.; Hu, S.; Zhu, D.; Li, J.; Cheng, K.; Liu, G. Comparison of extruded cell nanovesicles and exosomes in their molecular cargos and regenerative potentials. *Nano Res.* **2023**, *16*, 7248−7259.

(13) Bheri, S.; Hoffman, J. R.; Park, H. J.; Davis, M. E. Biomimetic nanovesicle design for cardiac tissue repair. *Nanomedicine (Lond)* **2020**, *15*, 1873−1896.

(14) Khan, M.; Kishore, R. Stem Cell Exosomes: Cell-FreeTherapy for Organ Repair. *Methods Mol. Biol.* **2017**, *1553*, 315−321.

(15) Qiao, L.; Hu, S.; Liu, S.; Zhang, H.; Ma, H.; Huang, K.; Li, Z.; Su, T.; Vandergriff, A.; Tang, J.; Allen, T.; Dinh, P. U.; Cores, J.; Yin, Q.; Li, Y.; Cheng, K. microRNA-21−5p dysregulation in exosomes derived from heart failure patients impairs regenerative potentia. *J. Clin Invest* **2019**, *129*, 2237−2250.
(16) Gallet, R.; Dawkins, J.; Valle, J.; Simsolo, E.; de Couto, G.; Middleton, R.; Tseliou, E.; Luthringer, D.; Kreke, M.; Smith, R. R.; Marbán, L.; Ghaleb, B.; Marbán, E. Exosomes secreted by cardiosphere-derived cells reduce scarring, attenuate adverse remodelling, and improve function in acute and chronic porcine myocardial infarction. *Eur. Heart J.* **2016**, *38*, 201−211.
(17) Zhang, E.; Liu, Y.; Han, C.; Fan, C.; Wang, L.; Chen, W.; Du, Y.; Han, D.; Arnone, B.; Xu, S.; Wei, Y.; Mobley, J.; Qin, G. Visualization and Identification of Bioorthogonally Labeled Exosome Proteins Following Systemic Administration in Mice. *Front Cell Dev Biol.* **2021**, *9*, 657456.
(18) Sahoo, S.; Adamiak, M.; Mathiyalagan, P.; Kenneweg, F.; Kafert-Kasting, S.; Thum, T. Therapeutic and Diagnostic Translation of Extracellular Vesicles in Cardiovascular Diseases: Roadmap to the Clinic. *Circulation* **2021**, *143*, 1426−1449.
(19) Liu, B.; Lee, B. W.; Nakanishi, K.; Villasante, A.; Williamson, R.; Metz, J.; Kim, J.; Kanai, M.; Bi, L.; Brown, K.; Di Paolo, G.; Homma, S.; Sims, P. A.; Topkara, V. K.; Vunjak-Novakovic, G. Cardiac recovery via extended cell-free delivery of extracellular vesicles secreted by cardiomyocytes derived from induced pluripotent stem cells. *Nat. Biomed Eng.* **2018**, *2*, 293−303.
(20) Tang, J.; Su, T.; Huang, K.; Dinh, P. U.; Wang, Z.; Vandergriff, A.; Hensley, M. T.; Cores, J.; Allen, T.; Li, T.; Sproul, E.; Mihalko, E.; Lobo, L. J.; Ruterbories, L.; Lynch, A.; Brown, A.; Caranasos, T. G.; Shen, D.; Stouffer, G. A.; Gu, Z.; Zhang, J.; Cheng, K. Targeted repair of heart injury by stem cells fused with platelet nanovesicles. *Nat. Biomed Eng.* **2018**, *2*, 17−26.
(21) Li, Z.; Hu, S.; Huang, K.; Su, T.; Cores, J.; Cheng, K. Targeted anti-IL-1beta platelet microparticles for cardiac detoxing and repair. *Sci. Adv.* **2020**, *6*, 589.
(22) Su, T.; Huang, K.; Ma, H.; Liang, H.; Dinh, P. U.; Chen, J.; Shen, D.; Allen, T. A.; Qiao, L.; Li, Z.; Hu, S.; Cores, J.; Frame, B. N.; Young, A. T.; Yin, Q.; Liu, J.; Qian, L.; Caranasos, T. G.; Brudno, Y.; Ligler, F. S.; Cheng, K. Platelet-Inspired Nanocells for Targeted Heart Repair After Ischemia/Reperfusion Injury. *Adv. Funct Mater.* **2019**, *29*, 1803567.
(23) Hu, S.; Wang, X.; Li, Z.; Zhu, D.; Cores, J.; Wang, Z.; Li, J.; Mei, X.; Cheng, X.; Su, T.; Cheng, K. Platelet membrane and stem cell exosome hybrid enhances cellular uptake and targeting to heart injury. *Nano Today* **2021**, *39*, 101210.
(24) Li, Q.; Huang, Z.; Pang, Z.; Wang, Q.; Gao, J.; Chen, J.; Wang, Z.; Tan, H.; Li, S.; Xu, F.; Chen, J.; Liu, M.; Weng, X.; Yang, H.; Song, Y.; Qian, J.; Ge, J. Targeted delivery of platelet membrane modified extracellular vesicles into atherosclerotic plaque to regress atherosclerosis. *CHEM ENG J.* **2023**, *452*, 138992.
(25) Wei, Z.; Qiao, S.; Zhao, J.; Liu, Y.; Li, Q.; Wei, Z.; Dai, Q.; Kang, L.; Xu, B. miRNA-181a over-expression in mesenchymal stem cell-derived exosomes influenced inflammatory response after myocardial ischemia-reperfusion injury. *Life Sci.* **2019**, *232*, 116632.
(26) Igarashi, K.; Ochiai, K.; Itoh-Nakadai, A.; Muto, A. Orchestration of plasma cell differentiation by Bach2 and its gene regulatory network. *Immunol Rev.* **2014**, *261*, 116−125.
(27) Shen, T.; Xia, L.; Dong, W.; Wang, J.; Su, F.; Niu, S.; Wang, Q.; Fang, Y. A Systematic Review and Meta-Analysis: Safety and Efficacy of Mesenchymal Stem Cells Therapy for Heart Failure. *Curr. Stem Cell Res. Ther* **2021**, *16*, 354−365.
(28) Thompson, M.; Mei, S. H. J.; Wolfe, D.; Champagne, J.; Fergusson, D.; Stewart, D. J.; Sullivan, K. J.; Doxtator, E.; Lalu, M.; English, S. W.; Granton, J.; Hutton, B.; Marshall, J.; Maybee, A.; Walley, K. R.; Santos, C. D.; Winston, B.; McIntyre, L. Cell therapy with intravascular administration of mesenchymal stromal cells continues to appear safe: An updated systematic review and meta-analysis. *EClinicalMedicine* **2020**, *19*, 100249.
(29) Li, J.; Sun, S.; Zhu, D.; Mei, X.; Lyu, Y.; Huang, K.; Li, Y.; Liu, S.; Wang, Z.; Hu, S.; Lutz, H. J.; Popowski, K. D.; Dinh, P. C.; Butte, A. J.; Cheng, K. Inhalable Stem Cell Exosomes Promote Hear Repair After Myocardial Infarction. *Circulation* **2024**, *150*, 710−723.
(30) Li, Z.; Hu, S.; Huang, K.; Su, T.; Cores, J.; Cheng, K. Targeted anti-IL-1β platelet microparticles for cardiac detoxing and repair. *Sci. Adv.* **2020**, *6* (6), No. eaay0589, Feb 5.
(31) Li, Y.; Yu, J.; Cheng, C.; Chen, W.; Lin, R.; Wang, Y.; Cui, W.; Meng, J.; Du, J.; Wang, Y. Platelet and Erythrocyte Membranes Coassembled Biomimetic Nanoparticles for Heart Failure Treatment. *ACS Nano* **2024**, *18*, 26614−26630.
(32) Li, Q.; Huang, Z.; Wang, Q.; Gao, J.; Chen, J.; Tan, H.; Li, S.; Wang, Z.; Weng, X.; Yang, H.; Pang, Z.; Song, Y.; Qian, J.; Ge, J. Targeted immunomodulation therapy for cardiac repair by platelet membrane engineering extracellular vesicles via hitching peripheral monocytes. *Biomaterials* **2022**, *284*, 121529.
(33) Cui, X.; Guo, J.; Yuan, P.; Dai, Y.; Du, P.; Yu, F.; Sun, Z.; Zhang, J.; Cheng, K.; Tang, J. Bioderived Nanoparticles for Cardiac Repair. *ACS Nano* **2024**, *18*, 24622−24649.
(34) Li, J.; Sun, S.; Zhu, D.; Mei, X.; Lyu, Y.; Huang, K.; Li, Y.; Liu, S.; Wang, Z.; Hu, S.; Lutz, H. J.; Popowski, K. D.; Dinh, P. C.; Butte, A. J.; Cheng, K. Inhalable Stem Cell Exosomes Promote Hear Repair After Myocardial Infarction. *Circulation* **2024**, *150*, 710−723.
(35) Liu, X.; Chen, B.; Chen, J.; Wang, X.; Dai, X.; Li, Y.; Zhou, H.; Wu, L. M.; Liu, Z.; Yang, Y. A Cardiac-Targeted Nanozyme Interrupts the Inflammation-Free Radical Cycle in Myocardial Infarction. *Adv. Mater.* **2024**, *36*, No. e2308477.
(36) Weng, H.; Zou, W.; Tian, F.; Xie, H.; Liu, A.; Liu, W.; Liu, Y.; Zhou, N.; Cai, X.; Wu, J.; Zheng, Y.; Shu, X. Inhalable cardiac targeting peptide modified nanomedicine prevents pressure erload heart failure in male mice. *Nat. Commun.* **2024**, *15*, 6058.
(37) Zhu, J.; Yao, K.; Guo, J.; Shi, H.; Ma, L.; Wang, Q.; Liu, H.; Gao, W.; Sun, A.; Zou, Y.; Ge, J. miR-181a and miR-150 regulate dendritic cell immune inflammatory responses and cardiomyocyte apoptosis via targeting JAK1-STAT1/c-FOS pathway. *J. Cell Mol. Med.* **2017**, *21*, 2884−2895.
(38) Ichiyama, K.; Long, J.; Kobayashi, Y.; Horita, Y.; Kinoshita, T.; Nakamura, Y.; Kominami, C.; Georgopoulos, K.; Sakaguchi, S. Transcription factor Ikzf1 associates with Foxp3 to repress gene expression in Treg cells and limit autoimmunity and anti-tumor immunity. *Immunity.* **2024**, *57*, 2043−2060.
(39) Nam, H. Y.; Kim, J.; Kim, S. W.; Bull, D. A. Cell targeting peptide conjugation to siRNA polyplexes for effective gene silencing in cardiomyocytes. *Mol. Pharmaceutics* **2012**, *9*, 1302−9.
(40) Nabhan, M.; Louka, M. L.; Khairy, E.; Tash, F.; Ali-Labib, R.; El-Habashy, S. MicroRNA-181a and its target Smad 7 as potential biomarkers for tracking child acute lymphoblastic leukemia. *Gene* **2017**, *628*, 253−258.
(41) Hannemann, N.; Jordan, J.; Paul, S.; Reid, S.; Baenkler, H.-W.; Sonnewald, S.; Bauerle, T.; Vera, J.; Schett, G.; Bozec, A. The AP-1 Transcription Factor c-Jun Promotes Arthritis by Regulating Cyclo-oxygenase-2 and Arginase-1 Expression in Macrophages. *J. Immunol* **2017**, *198*, 3605−3614.

https://doi.org/10.1021/acsami.4c19325
ACS Appl. Mater. Interfaces 2025, 17, 16520−16532